Biosensors and Bioelectronics 85 (2016) 977–985

Contents lists available at ScienceDirect

Biosensors and Bioelectronics

journal homepage: www.elsevier.com/locate/bios

Sensitivity improvement of an electrical sensor achieved by control of biomolecules based on the negative dielectrophoretic force

Hye Jin Kim [a,b,1], Jinsik Kim [a,1], Yong Kyoung Yoo [a], Jeong Hoon Lee [c], Jung Ho Park [b], Kyo Seon Hwang [a,*]

[a] Center for Biomicrosystems, Korea Institute of Science and Technology (KIST), Hwarang-ro 14-gil 5, Seongbuk-gu, Seoul 02792, Republic of Korea
[b] Department of Electrical Engineering, Korea University,145 Anam-ro, Seongbuk-gu, Seoul 02841, Republic of Korea
[c] Department of Electrical Engineering, Kwangwoon University, 20 Gwangun-ro, Nowon-gu, Seoul 01897, Republic of Korea

ARTICLE INFO

Article history:
Received 28 April 2016
Received in revised form
21 June 2016
Accepted 27 June 2016
Available online 28 June 2016

Keywords:
Sensitivity
Limit of detection
Dielectrophoresis
Electrical sensor
Immunochemical method

ABSTRACT

Effective control of nano-scale biomolecules can enhance the sensitivity and limit of detection of an interdigitated microelectrode (IME) sensor. Manipulation of the biomolecules by dielectrophoresis (DEP), especially the negative DEP (nDEP) force, so that they are trapped between electrodes (sensing regions) was predicted to increase the binding efficiency of the antibody and target molecules, leading to a more effective reaction. To prove this concept, amyloid beta 42 ($A\beta_{42}$) and prostate specific antigen (PSA) protein were respectively trapped between the sensing region owing to the nDEP force under 5 V and 0.05 V, which was verified with COMSOL simulation. Using the simulation value, the resistance change ($\Delta R/R_b$) of the IME sensor from the specific antibody–antigen reaction of the two biomolecules and the change in fluorescence intensity were compared in the reference (pDEP) and nDEP conditions. The $\Delta R/R_b$ value improved by about 2-fold and 1.66-fold with nDEP compared to the reference condition with various protein concentrations, and these increases were confirmed with fluorescence imaging. Overall, nDEP enhanced the detection sensitivity for $A\beta_{42}$ and PSA by 128% and 258%, respectively, and the limit of detection improved by up to 2-orders of magnitude. These results prove that DEP can improve the biosensor's performance.

1. Introduction

Sensitivity enhancement is the most critical factor to achieve a powerful sensor. A variety of approaches have been applied to develop a sensor with higher performance such as miniaturizing the size of the sensor (Gerwen et al., 1998; Derkus, 2016; Hsueh and Lin, 2016), and applying a two-dimensional (2D) or three-dimensional (3D) porous structure to increase the reaction area-to-volume ratio (Zhu et al., 2015; Song et al., 2016). Furthermore, utilization of electrokinetics by application of an electric field on an electrode has been demonstrated to improve a sensor's performance. Electrokinetics such as alternative current (AC)-dielectrophoresis (DEP) and AC-electroosmosis (EO) were originally applied to trap, sort, or separate a nano- and micro-particle in liquid (Ramos et al., 1998; Jones, 1995). Because of their potential for preconcentrating during the trapping of biomolecules, DEP and EO have been applied to enhance a sensor's performance as a simpler alternative to the more time- and cost-consuming methods such as miniaturizing the sensor or utilization of additional structures.

Various biomolecules such as proteins and bacteria that are present in low amounts in a sample have been measured with preconcentration of a sensor by DEP or EO (Dastider et al., 2016; Gong, 2010). By using the positive DEP (pDEP) force, the bacterium *E. coli* O157:H7, which has a diameter of about ~1 μm, was detected at sub-hundreds of colony forming units (Dastider et al., 2016). Although this system showed a quite low limit of detection (LOD), an additional complex structure was nevertheless required to induce the trapping force, and the detected material (bacteria) was much larger than typical biomolecules. The measurement of prostate specific antigen (PSA), which is a considerably smaller molecule than bacteria, was also effectively measured in amounts below sub-ten femtograms per milliliter with EO (Gong, 2010). However, in this case, a nano-wire type sensor was used, which has low reliability and involves a costly fabrication method. Furthermore, in both examples above, the strong attractive force was used, which can cause undesirable defects when trapping target biomolecules (Kim et al., 2013). Although research in this field has led to dramatic enhancement of the sensitivity and LOD of electric sensors, a sensor with a simpler structure and fabrication method

* Corresponding author.
E-mail address: kshwang@kist.re.kr (K.S. Hwang).
[1] H.J. Kim and J. Kim contributed equally to this work.

http://dx.doi.org/10.1016/j.bios.2016.06.081
0956-5663/

is required for various biological applications to conform with increasing awareness of the importance of "point-of-care" testing (Fang et al., 2009; Chen et al., 2013), mainly based on high sensitivity and LOD.

In this study, an IME sensor was developed, which has ultra-high sensitivity and a low LOD that was achieved through pre-concentrating the target between electrodes by a negative DEP (nDEP). The performance of the sensor was tested with detection of amyloid beta 42 (4.5 kDa) and PSA (34 kDa) to show its variable applications for the detection of a wide range of biomolecules. Amyloid beta 42 and PSA are crucial biomarkers for Alzheimer's disease and prostate cancer, respectively. To simplify the structure of the sensor, the sensing electrode of the IME and the biomolecules-manipulating electrode with DEP were designed to be unified. The nDEP was also utilized to increase the concentration of biomolecules at the reaction region so that non-specific binding was reduced by ensuring the manipulation of only target molecules. The IME sensor was fabricated with micro-electro-mechanical systems (MEMS) technology, and the conditions of inducing nDEP were determined with COMSOL multiphysics simulation. The change of resistance ($\Delta R/R_b$) of the IME sensor caused by a specific reaction of amyloid beta 42 and PSA was measured in each DEP condition to verify the calculated conditions. Finally, enhancement of the sensitivity and LOD by nDEP was also accomplished through analysis of the $\Delta R/R_b$ and fluorescence intensity according to the concentration of each type of biomolecule tested.

2. Material and methods

The DEP force induced by an applied AC voltage can be trapped to focus the biomolecules between the IME sensor's electrodes. Therefore, the resistance of the sensor would be expected to change according to the presence of the DEP force, and thus the performance of the sensor can be improved. This concept to improve the performance of a sensor with DEP is shown schematically in Fig. 1. A non-uniform field (E-field) induced by the AC voltage in two parallel electrodes causes the DEP force (Fig. 1(a)). Because the force influences the nano-molecules suspended in the E-field, the molecules are controlled by the DEP force. The DEP force can be classified into pDEP and nDEP, and the motion of molecules is influenced by the type of force applied (Fig. 1(b)). The inset of Fig. 1(c) shows the expected change of the resistance over time in each condition before and after the reaction.

Without any AC voltage ("*(1) Reference*" in Fig. 1(b)), the biomolecules affect only Brownian motion. Therefore, the molecules randomly suspended in buffer show a steady concentration regardless of time and position. However, when the AC voltage is applied to the sensor, the concentration of biomolecules close to the electrodes changes owing to the influence of the DEP force. In the pDEP condition, the biomolecules are focused at the surface of the electrode because the pep force is formed toward the maximum electric field gradient region ("*(2) Positive DEP*" in Fig. 1(b)). The focused biomolecule causes only slight increase of resistance compared to that in the reference condition (green spots in Fig. 1(c)). By contrast, the dip force is induced toward the region with the minimum electric field gradient, and, consequently, the biomolecules are trapped and arranged between the electrodes ("*(3) Negative DEP*" in Fig. 1(b)). Thus, the arranged biomolecules show a greater change in resistance compared to the reference condition (red spots in Fig. 1(c)).

2.1. Fabrication of the IME sensor

The IME sensor was fabricated using standard micro-fabrication techniques (Fig. S1). An SiO_2 layer, with a thickness of 300 nm, was grown on a 4-inch silicon (Si) wafer by thermal deposition. Tantalum (Ta) and platinum (Pt) were sequentially deposited at a thickness of 30 nm and 150 nm, respectively, on the SiO_2 layer by sputtering. The photoresist (PR) AZ GXR 601 (AZ electronic materials) was spin-coated on the wafer at 3000 rpm, exposed to UV light (3.8 s, 12 mW cm^{-2}) via a photomask after baking at 95 °C for 60 s, and then developed. The electrode pattern was formed by inductively coupled plasma etching (Oxford Instruments) after baking at 120 °C for 3 min. The PR was removed using Microwave Plasma Asher (Plasma Finish). A single chip with a width of 10 mm and length of 24 mm was composed of six IME sensors. One IME sensor consisted of 30 pairs of microelectrode fingers, which were interdigitated with spacing of a 5 μm width and 300 μm length. (Fig. 2(a)) The fabricated sensor was bonded with a polydimethlysiloxane (PDMS, Sylgard, Dow Corning) channel by the van der Waals force for the immunoassay. The fabrication process of the PDMS channel is described in the Supplementry information.

2.2. Surface functionalization of the IME sensor for the immunoassay

For immobilization of the antibody, the IME sensor was sequentially washed using piranha solution (H_2SO_4:H_2O_2=4:1), deionized water, and isopropanol alcohol (IPA, Danjung Chemicals & Metals, Siheung, Korea) to remove the organic and inorganic residues. The surface of the SiO_2 was functionalized by 1% (3-aminopropyl)triethoxysilane (Sigma-Aldrich, St. Louis, MO, USA) solution in IPA for 3 h, followed by washing with pure IPA and 100 mM sodium bicarbonate ($NaHCO_3$, Sigma-Aldrich, St. Louis, MO, USA) buffer (pH 9.0). The IME sensor was transferred to 2 mM of poly(N-vinylpyrrolidone) with an aldehyde end-group (PVP-CHO) solution in $NaHCO_3$ buffer overnight, rinsed with $NaHCO_3$ buffer, and the aldehyde group on the sensor's surface was reduced using 10 mM sodium borohydride ($NaBH_4$, Sigma-Aldrich, St. Louis, MO, USA) for 1 h. Then, the IME sensor was washed with $NaHCO_3$ buffer. The reduced surface was functionalized by 1% glutaraldehyde solution in $NaHCO_3$ buffer for 1 h and rinsed sequentially with $NaHCO_3$ buffer and 1x phosphate-buffered saline (PBS, pH 7.4). Following the functionalization, 10 μg mL^{-1} antibody in 1 × PBS buffer was immobilized on the SiO_2 surface and incubated for 1 h for covalent bonding. The excess antibodies were washed away by rinsing with pure 1 × PBS buffer. All procedures for surface modification were carried out at room temperature and confirmed with measurement of fluorescent images, as shown in Fig. S2.

2.3. Immunoassay process

The immunoassay process was composed of 4 steps (Fig. 2(b)). First, 20 μL of 1X PBS buffer was injected in the PDMS channel by a syringe and the initial resistance of the IME sensor (R_b) was measured. Then, 40 μL of 1 × PBS solution with the target protein was injected into the PDMS channel and the AC voltage was applied to cause the DEP force using a function generator, while the antibody immobilized on the sensor's surface was reacted with the target molecules. In this step, the target molecule was moved by the external force. The applied frequency and AC voltage are expressed as f_a and V_a, respectively. After the reaction, the IME sensor was rinsed with 300 μL of 1 × PBS buffer to minimize the resistance change by the non-specific binding. Finally, the resistance was measured in 1 × PBS buffer (R_a). The specific binding between the antibody and target molecules was demonstrated by the signal difference of resistance before and after the reaction, defined as $\Delta R = R_a - R_b$. All immunoassay steps were conducted at room temperature. For the immunoassay, the 6E10 (Purified anti-β-Amyloid antibody, 1-16, BioLegend, San Diego, CA, USA)

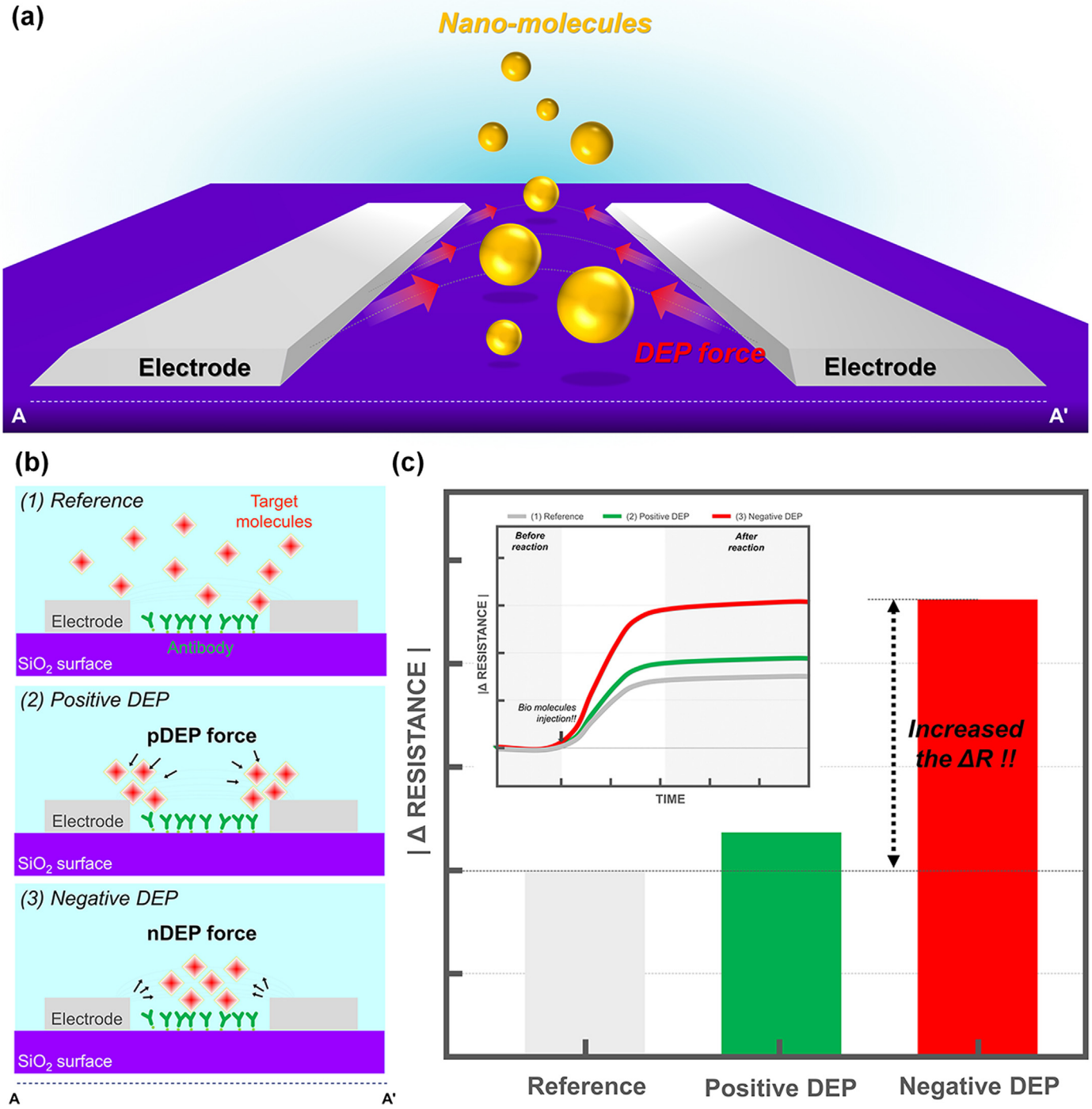

Fig. 1. (a) Schematic representation of the concept for enhancing the performance of a sensor by controlling the nano-scale molecules with the DEP force. (b) The motion of the nano-molecules in a non-uniform E-field according to the type of DEP force. (c) The change of resistance before and after the reaction of biomolecules in the reference (gray), pDEP (green), and nDEP (red) condition. The inset shows the change of resistance over time. (For interpretation of the references to color in this figure legend, the reader is referred to the web version of this article.)

antibody and the M612166 antibody (Anti-PSA antibody, Fitzgerald, MA, USA) were used. In addition, amyloid beta protein fragment 1–42 (Sigma-Aldrich, St. Louis, MO, USA), a fluorescent-tagged amyloid beta protein (β-Amyloid (1-42), TAMRA-labeled, AnaSpec, Fermont, USA) and PSA protein (Fitzgerald, MA, USA) were used as the specific binding targets for each antibody. An electron-multiplying charge-coupled device (ANDOR iXonEM), an oil immersion 100× lens (NA: 1.4, Nikon), and a microscope (Eclipse Ti, Nikon) were used to confirm the nano-molecules on the IME sensor with a halogen lamp and a 593-nm (bandwidth: 40 nm) filter to detect the fluorescent light signal of the nano-particles. The fluorescence images were processed using Image J (ver. 4.5) software to magnify the images for efficiently showing of fluorescent signals from narrow dimension of IME. Fluorescence images were relatively compared without additional processing after the magnifying were used for analysis.

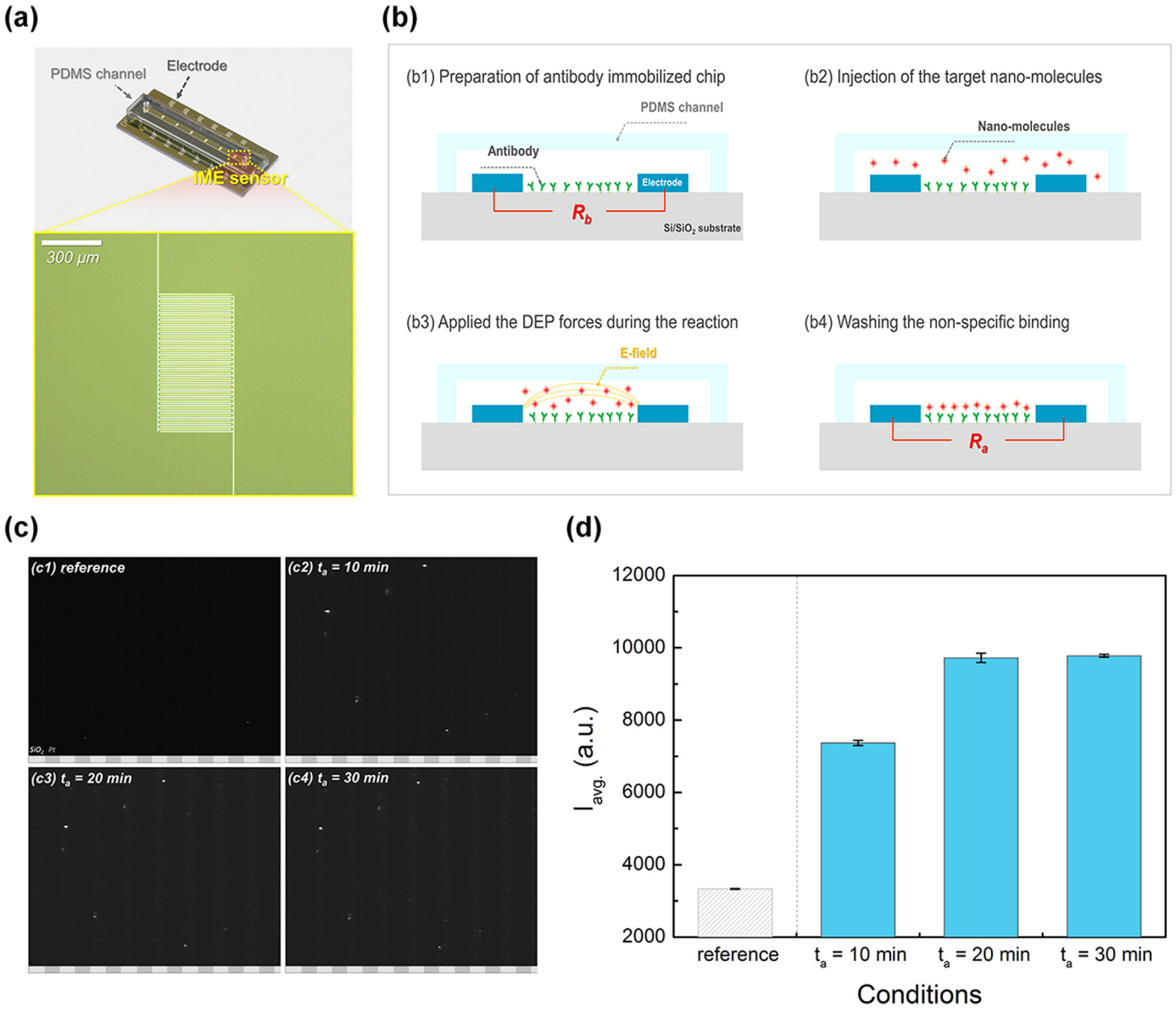

Fig. 2. (a) The fabricated IME sensor using MEMS technology. (b) Illustration of the experimental process used to detect the biomolecules. R_b and R_a is the resistance measured before and after detection of the antibody and biomolecules.

3. Results and discussion

3.1. Modeling and simulation

The IME sensor was composed of a sensing region (the IME's fingers and SiO_2) and an electrode pad (Fig. 2(a)). The fingers consisted of 30 pairs of electrodes spaced at regular intervals and could detect the change in resistance by the binding of the biomolecules between the electrodes. The molecules reacted with the antibody on the SiO_2 surface functionalized by chemical treatment. By contacting the electrode pad with the external probe, it was possible to apply the AC voltage for the DEP force and to measure the change in resistance.

The damping force caused by viscosity of the liquid was calculated by Stokes' Law and was expressed by the dynamic viscosity of the medium and the velocity of the molecules in the buffer. The relationship between the DEP and damping force was described with the acceleration and mass of the target molecules in two dimensions. By solving the equation, the velocity of suspended molecules by the external force, υ, can be predicted, and the position of the trapped molecules can be calculated according to the applied voltage. To calculate the DEP force, the gradient value of the electric field square, $\nabla|E|^2$, was predicted by simulation, as shown in Fig. S3. The IME sensor was simulated using the two-dimensional AC/DC module of COMSOL Multiphysics software (version 4.2). The IME sensor was modified with two electrodes with a gap of 5 μm and thickness of 0.15 nm. The distributed impedance boundary conditions were set along the sides and top of the modeled electrode, and the bottom surface was set as an electrically insulating boundary.

As the AC voltage was applied to the electrode, the suspended molecules around the electrode affected the DEP force, and the reverse force against the DEP force was simultaneously induced on the molecules by liquid damping. The DEP force caused the motion of suspended molecules at certain directions, which was impeded by the reverse force. Thus, the position of the suspended molecules was settled through the combination of the motion force and hindrance force by DEP and damping, respectively. In the nDEP

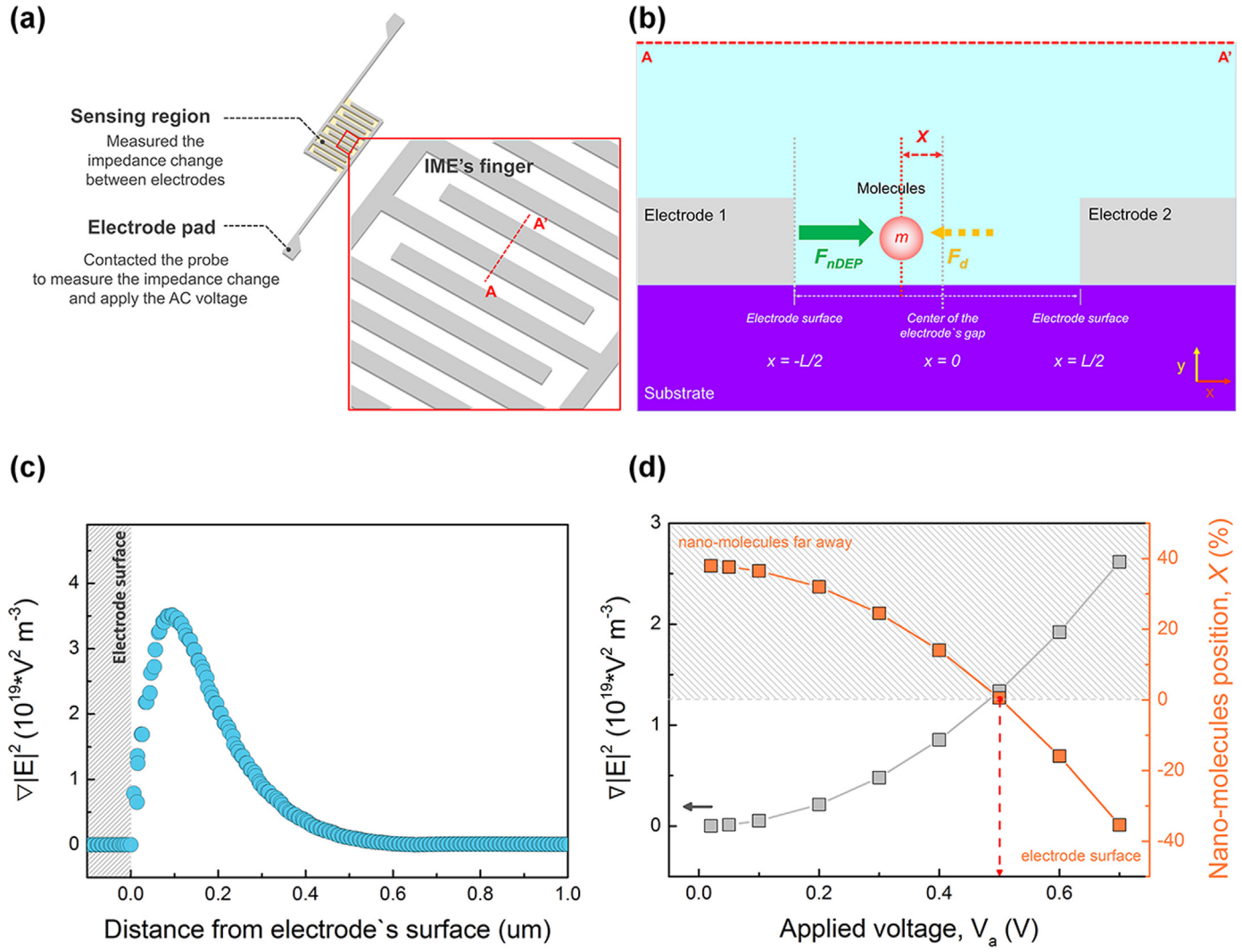

Fig. 3. Schematic illustration of (a) the IME sensor and (b) two forces that affect the position of nano-molecules between the electrodes in buffer. The position of the nano-molecules with mass "m" is shown as the red particle designated "X". The green and yellow arrows show the DEP force and damping force, respectively. (c) Predicted E-field at 0.8 V according to the distance from the electrode's surface. (d) The E-field (gray) and position (orange) of nano-molecules induced by the applied voltage (V_a). The size of the nano-molecules was set to 4.5 kDa. (For interpretation of the references to color in this figure legend, the reader is referred to the web version of this article.)

condition, the pushing force from the electrode surface induced by nDEP (F_{DEP}, green arrow in Fig. 3(b)) and the hindrance force by damping (F_d, yellow arrow in Fig. 3(b)) determined the location of the suspended molecules so that the target molecules were trapped between the electrodes. The position of molecules between an electrode's gap "L" with mass "m" is defined as "X". The F_{DEP} is defined according to Eq. (1) (Ramos et al., 1998; Jones, 1995):

$$F_{DEP}=2\pi\epsilon_m r^3 Re\left[K(\omega)\right]\nabla|E|^2 \quad (1)$$

where ε_m, r, ω, and E are the relative medium permittivity, particle radius, angular frequency, and electric field strength, respectively. K(ω) is the Clausius-Mossotti factor (CM) (Jin et al., 2016), which changed by the "crossover frequency" (Morgan and Green, 2001) from −0.5 to 1.0. These values confirmed that the nDEP and pDEP force occurred (i.e., the negative CM factor led to the nDEP force).

3.2. Optimization of the DEP voltage

For the simulation, amyloid β protein and 1× PBS were used, and the electrode was applied at 0.8 V. The $\nabla|E|^2$ showed a maximum intensity of about $\sim 10^{19}$ V^2 m^{-3} at 0.1 μm from the electrode surface and decreased exponentially (Fig. 3(c)). The maximum intensity inside the 0.1 μm range is the impetus to control the position of the biomolecules. Using the $\nabla|E|^2$,the position of the biomolecules (X) according to the applied voltage (V_a) was calculated (Fig. 3(d)). On the right y-axis, X (orange line) is zero at the center of the gap between the two electrodes and ranged from −50 to 50 (X shows a minimum and maximum value at each left and right electrode surface). The X of the nano-molecules located around the surface of the electrode had a negative value with low V_a, because the nano-molecules were hardly affected by the DEP force. Namely, they were suspended in the buffer randomly. By contrast, at high V_a, the nano-molecules flew out of the E-field owing to the strong pushing force exerted from both sides. Namely, the molecules were ejected between the electrodes if the E-field (gray dashed region in Fig. 3(d)) was applied. The optimum value required for the biomolecule to be located at the center of the electrode was calculated to be 0.5 V. The conditions of applied frequency (f_a) required to induce each nDEP and pDEP force were fixed at 1 MHz and 50 MHz, and the reaction time (t_a) was fixed to 20 min. The optimization process for each condition is described in the Supplemntary information.

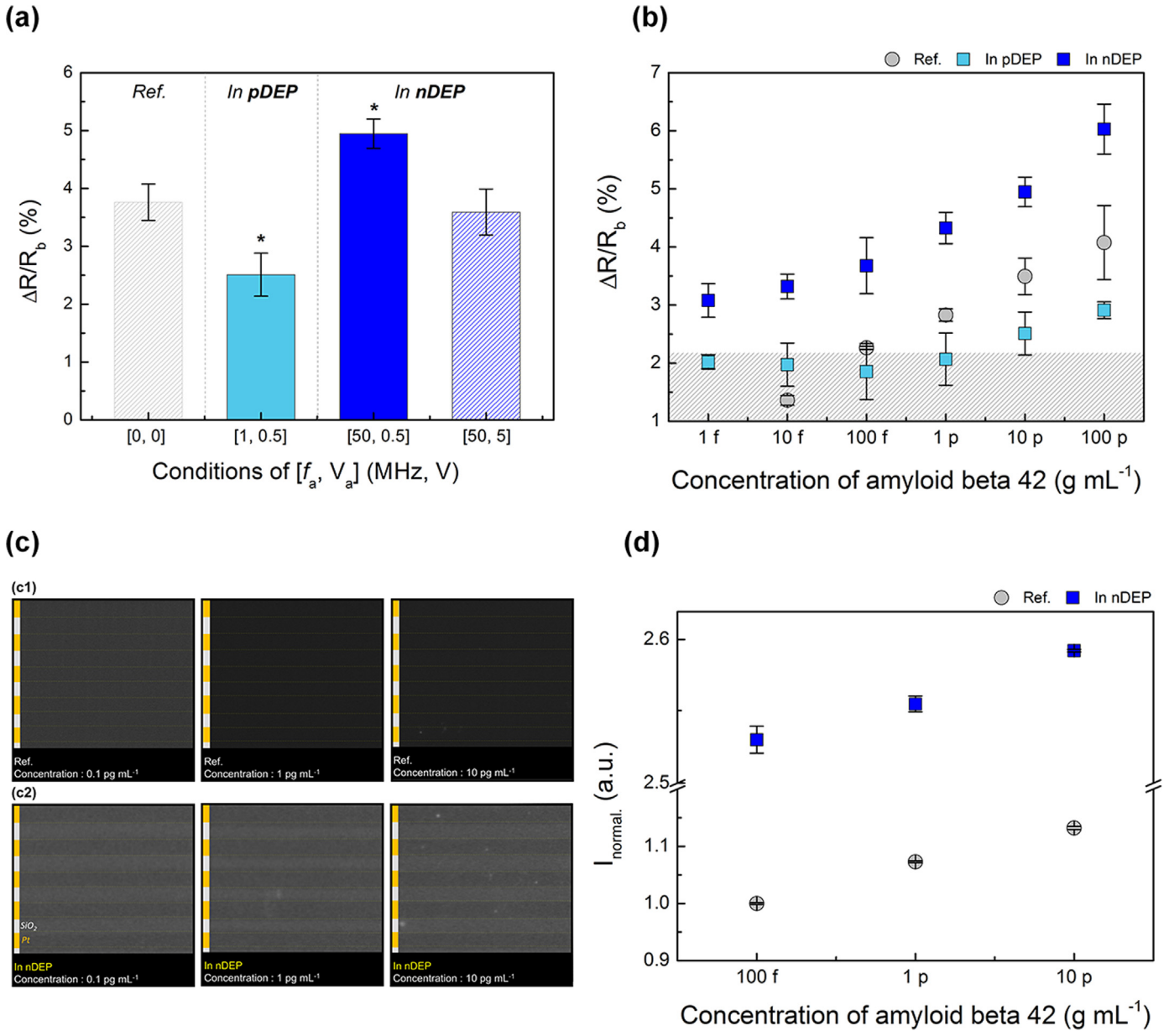

Fig. 4. Amyloid beta 42 protein detection to verify the effect of the DEP force. (a) Optimization of DEP conditions by measuring the change of resistance ($\Delta R/R_b$) in each DEP condition. The $\Delta R/R_b$ in the left region of the graph is the result in the reference condition ("Ref.") and the $\Delta R/R_b$ in the center and right regions of the graph are the effects by the pDEP and nDEP force, respectively ("In pDEP" and "In nDEP"). (b) The change of $\Delta R/R_b$ by reaction of 6E10 antibody and amyloid beta 42 protein in the reference (light gray), pDEP (light blue), and nDEP (dark blue) condition. In each condition, the resistance was changed according to the change in concentration of amyloid beta 42 protein. (c) Fluorescence image of detection of amyloid beta 42 protein, and (d) average intensity of fluorescence on the SiO_2 surface in the reference condition and nDEP condition. The data represent mean values and the error bars are standard deviations. (For interpretation of the references to color in this figure legend, the reader is referred to the web version of this article.)

3.3. Detection of amyloid beta 42 protein

To verify an effect by the DEP force, the ΔR resulting from the reaction of amyloid beta protein was measured under four conditions (Fig. 4(a)). The 6E10 antibody was immobilized on the SiO_2 surface using a surface-functionalized process, and the concentration of amyloid beta protein fragment 1-42 with a size of 4.5 kDa used for the reaction was 10 pg mL^{-1} in 1X PBS buffer. The reaction time between the 6E10 antibody and amyloid beta protein was set to 20 min. The R of the IME sensor was measured at 1 kHz with four conditions of f_a (MHz) and V_a (V), expressed as [f_a, V_a]: [0,0], [1,5], [50, 0.5], and [50, 5], classified according to the f_a as the reference, pDEP, and nDEP condition. Because the biomolecules were affected differently by each force in the pDEP and nDEP conditions, the $\Delta R/R_b$ values were different. The $\Delta R/R_b$ caused by the specific binding was $3.76 \pm 0.31\%$ in the reference, $2.51 \pm 0.37\%$ in pDEP, and $4.95 \pm 0.23\%$ and $3.59 \pm 0.39\%$ in each. The $\Delta R/R_b$ value was smaller in the pDEP condition compared to the reference, because the pDEP force attracted the biomolecules to the immobilized antibody at the electrode surface and not at the SiO_2 surface. By contrast, the biomolecules were pushed and trapped near the antibody by the nDEP force in the nDEP condition at $V_a = 0.5$ V. Therefore, the $\Delta R/R_b$ was larger in the nDEP condition compared to the reference. However, the $\Delta R/R_b$ value was different within the nDEP condition when the intensity of the force varied. In nDEP of $V_a = 5$ V, the $\Delta R/R_b$ was similar to that of the reference, because the biomolecules were moved far away owing to the strong force pushing from both sides. Based on these

results, the $\Delta R/R_b$ was measured according to the concentration of amyloid beta 42 to verify the sensitivity at a concentration range of 1 fg mL^{-1} to 100 pg mL^{-1}. As shown in Fig. 4(a), the $\Delta R/R_b$ changed from $1.36 \pm 0.08\%$ to $4.08 \pm 0.64\%$ in the reference along with a change in amyloid beta 42 concentration from 10 fg mL^{-1} to 100 pg mL^{-1}. The $\Delta R/R_b$ increased from $1.97 \pm 0.37\%$ to $2.91 \pm 0.14\%$, and from $2.95 \pm 0.29\%$ to $6.03 \pm 0.43\%$ in the pDEP and nDEP condition, respectively, with a change in concentration from 1 fg mL^{-1} to 100 pg mL^{-1} (Fig. 4(b)). The value of $\Delta R/R_b$ obtained by non-specific binding was about $2.22 \pm 0.11\%$ (gray dashed region). Due to the change of $\Delta R/R_b$, the upper value was guaranteed to be the real signal caused by the specific binding, and the concentration in which the $\Delta R/R_b$ value overlapped with the gray dashed region was not detectable. Detailed information of this gray region is described in Fig. S1. In the reference condition, the $\Delta R/R_b$ overlapped with the gray region at an amyloid beta 42 concentration of 100 fg mL^{-1}. However, the $\Delta R/R_b$ did not overlap with this region in the nDEP condition, even at an amyloid beta 42 concentration of 1 fg mL^{-1}. Moreover, the intensity of $\Delta R/R_b$ was increased by about 2-fold from the nDEP force compared to the reference in general.

The effects of nDEP force by AC voltage with 50 MHz and 0.5 V_{pp} were also investigated with fluorescence microscopy. The images of a fluorescent-tagged amyloid beta protein concentration of 100 fg mL^{-1} to 10 pg mL^{-1} were compared in the reference and nDEP condition after the reaction (Fig. 4(c)). The fluorescent images were observed using a 50× lens at broad regions consisting of a dozen IME fingers. In the reference, the fingers were indistinguishable because the overall intensity of the image was low. However, increasing of the binding probability caused by nDEP brightened the signal, so that the fingers of the IME sensor could be clearly distinguished. Depending on the concentration of amyloid beta antigen, the overall intensity of the image was also increased. These trends were analyzed quantitatively using an image processing tool (Fig. 4(d)), and the intensity measured from five random positions was averaged to determine the normalized fluorescence intensity as the average intensity in each condition divided by a standard average intensity. The standard average intensity was the value in the reference condition with an amyloid beta protein concentration of 0.1 pg mL^{-1}. According to the concentration of amyloid beta 42, the normalized average intensity values were 1 ± 0.001, 1.073 ± 0.002, and 1.132 ± 0.003 in the reference condition, and were 2.529 ± 0.009, 2.555 ± 0.006, and 2.592 ± 0.001 in the nDEP condition The results showed a minimum 2.29-fold difference of the fluorescence intensity between the reference and nDEP condition. These results corresponded well to the observed resistance change with nDEP.

3.4. Detection of PSA protein

The DEP effects were measured with another biomolecule, PSA protein, to prove the universality of the concept proposed. PSA protein is about 7.5-times bigger than amyloid beta 42. Before detection of PSA protein, the optimum V_a condition was calculated to be 0.02 V using Eq (1). The M612166 antibody was used to detect the PSA protein, and was immobilized on the surface of SiO_2 by the same surface treatment protocol. The ΔR was measured in six conditions for [f_a, V_a] to determine the optimum condition. The six conditions, [0,0], [1, 0.2], [1, 5], [50, 0.02], [50, 0.1], [50, 0.1], and [50, 0.5], were applied for 20 min, and the ΔR caused by reaction of 1 pg mL^{-1} PSA protein was measured (Fig. 5(a)). The $\Delta R/R_b$ caused by specific binding was $2.08 \pm 0.21\%$ in the reference and $2.29 \pm 0.02\%$ and $2.33 \pm 0.16\%$ in each pDEP condition. In the nDEP condition, the $\Delta R/R_b$ was changed from $3.34 \pm 0.39\%$, $2.38 \pm 0.30\%$, and $2.29 \pm 0.50\%$ according to the increase of the V_a. Because the PSA protein was attracted to the surface of the electrode by the pDEP force, the $\Delta R/R_b$ showed a similar change as the reference, with little influence according to the V_a condition. By contrast, the PSA protein trapped between the electrodes in the nDEP condition led to an increase in the ΔR, and the $\Delta R/R_b$ was changed depending on the V_a condition. The $\Delta R/R_b$ induced by binding of PSA protein was largest in the condition of $V_a = 0.02$ V and decreased with the increase of the V_a because of the strong repulsive force applied from both sides of the electrode surface. According to these results, we measured the $\Delta R/R_b$ according to various concentrations of PSA protein (1 pg mL^{-1} to 1 ng mL^{-1}) in each DEP condition. In the reference, the $\Delta R/R_b$ increased from $2.08 \pm 0.21\%$ to $2.84 \pm 0.43\%$ in the PSA concentration range of 1 pg mL^{-1} to 1 ng mL^{-1}. The $\Delta R/R_b$ increased from $2.08 \pm 0.02\%$ to $3.62 \pm 0.13\%$ and from $2.94 \pm 0.13\%$ to $5.08 \pm 0.40\%$ in the pDEP and nDEP condition, respectively, with various concentrations of the PSA protein (Fig. 5(b)). The $\Delta R/R_b$ value for non-specific binding was about $2.11 \pm 0.23\%$ (gray dashed region; see Supplementary information for details). In the reference, the $\Delta R/R_b$ overlapped with

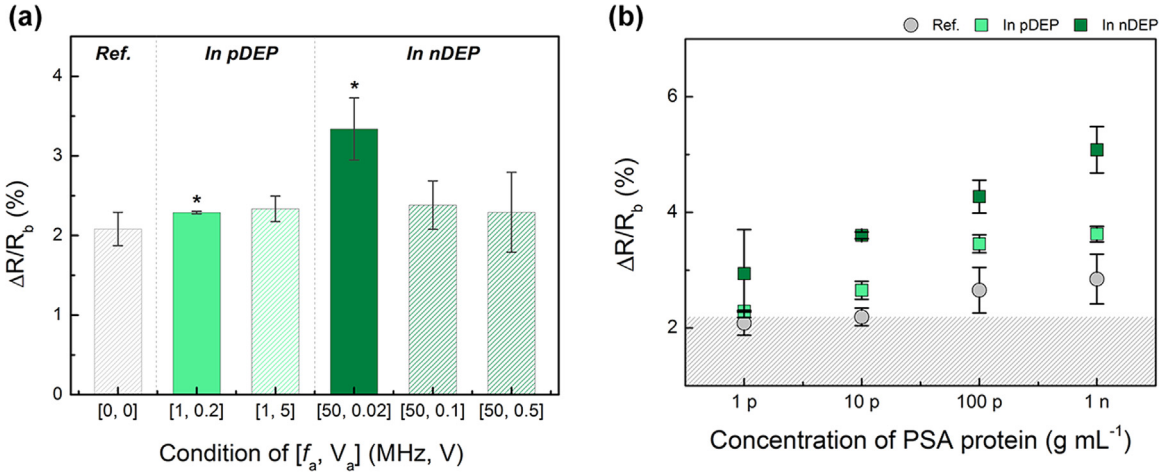

Fig. 5. Effect of DEP force on PSA protein detection. (a) Optimization of the DEP conditions by measuring the $\Delta R/R_b$ in each condition. The $\Delta R/R_b$ in the left, center, and right regions of the graph are the results in the reference, pDEP, and nDEP condition, respectively ("Ref.", "In pDEP", and "In nDEP"). (b) The detection results according to the concentration of PSA protein. The $\Delta R/R_b$ changed with the change in concentration of PSA protein in the reference (light gray), pDEP (light blue), and nDEP (dark blue) condition. (For interpretation of the references to color in this figure legend, the reader is referred to the web version of this article.)

the gray dashed region with a PSA concentration of 1 pg mL^{-1}, but no such overlap was observed for the same PSA concentration in the nDEP condition. Moreover, the $\Delta R/R_b$ was increased from about 1.52-fold to 1.79-fold by the nDEP compared to the reference with various concentrations of PSA.

3.5. Performance of the sensor

Using the two types of biomolecules (amyloid beta 42 protein and PSA protein), the effect of DEP in the IME sensor was confirmed. The nDEP force induced a repulsive force that trapped the biomolecules at the antibody-immobilized surface between the electrodes. Therefore, the IME sensor could detect lower concentrations of the biomolecules in a wider concentration range than possible with the reference condition.

The performance enhancement of the IME sensor conferred by nDEP was analyzed quantitatively by comparing the sensitivity and LOD in each condition. The sensitivity was measured as the change of the output signal according to the concentration of biomolecules, determined from the slope of the lines in Fig. 4 (b) and Fig. 5(b). The sensitivity for PSA detection was calculated as 0.28, 0.48, and 0.71 in the reference, pDEP, and nDEP condition, respectively. The sensitivity for amyloid beta detection was 0.58, 0.38, and 0.75 in the reference, pDEP, and nDEP condition, respectively. To verify the change in the sensitivity induced by DEP, the enhancement of sensitivity was calculated in comparison to the reference condition, which was set to 100% (Fig. 6(a)). For nDEP and pDEP, the sensitivity was respectively enhanced by 128% and 64% in the detection of amyloid beta 42, and by 258% and 175% in the detection of PSA protein. Thus, detection sensitivity of both biomolecules was improved by nDEP, although the specific enhancement value was different. The enhancement effect by pDEP also differed for the two biomolecules; pDEP reduced the sensitivity in amyloid beta detection, but increased the sensitivity in PSA detection. Consequently, pDEP reduced and increased the sensitivity for amyloid beta and PSA detection, respectively, compared to the reference. This difference is due to the molecular size dependency of the DEP force. Because the influence of DEP is more effective for bigger molecules, the sensitivity of PSA detection was more enhanced by the nDEP force than in the case of amyloid beta detection.

The LOD was also determined to evaluate the performance of the sensor for each biomolecule and condition. Because the $\Delta R/R_b$ was increased by about 2.22% by non-specific reaction at an amyloid beta 42 concentration greater than 100 fg mL^{-1}, the LOD was determined to be 100 fg mL^{-1} in the reference (Fig. 6(b)). By contrast, the $\Delta R/R_b$ in the detection of amyloid beta 42 was higher than the signal induced by the non-specific reaction at a concentration of 1 fg mL^{-1}. These results demonstrated that an IME sensor using nDEP could detect amyloid beta 42 at a concentration as low as 1 fg mL^{-1}. This enhancement in performance was also confirmed in PSA detection (Fig. 6(c)): the LOD was 10 pg mL^{-1} without nDEP, and improved to 1 pg mL^{-1} with nDEP.

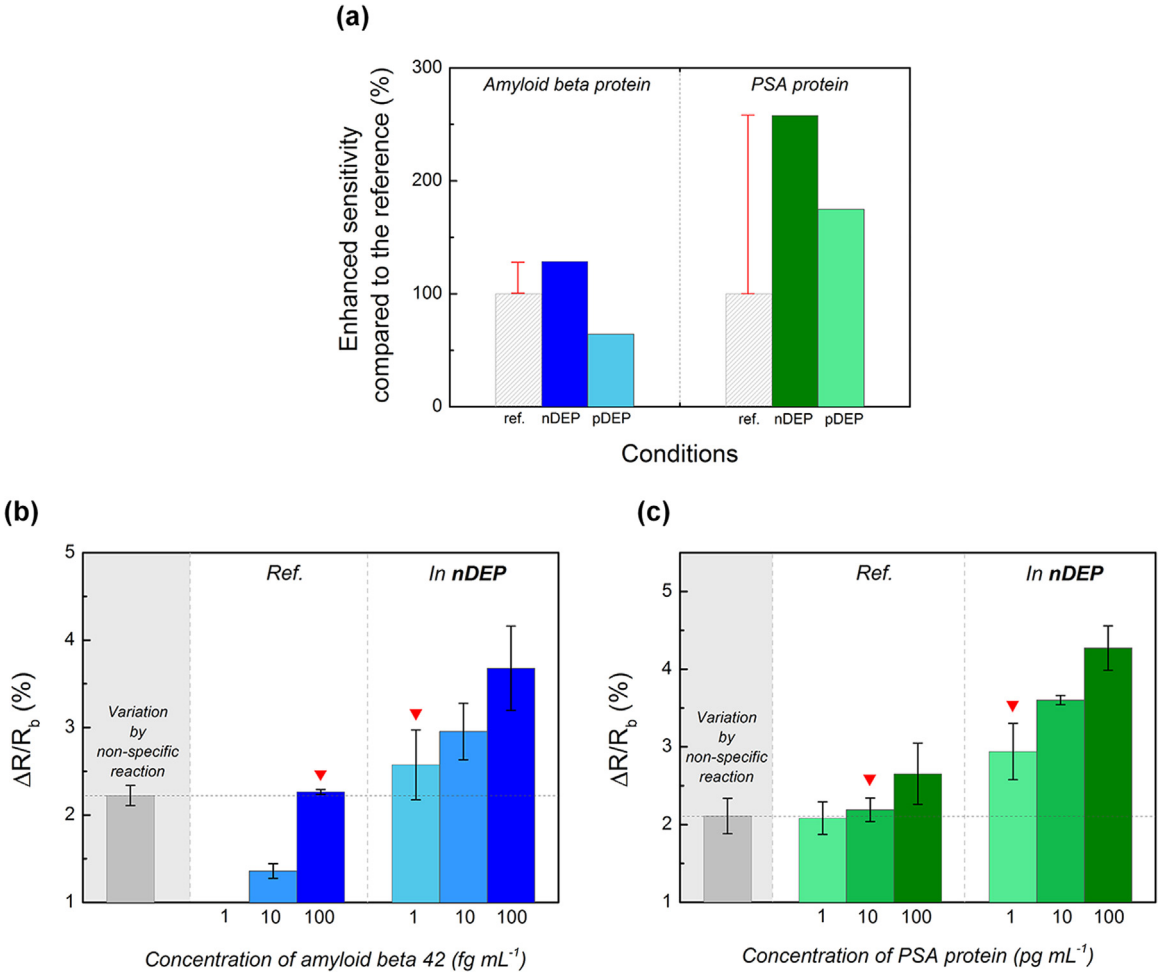

Fig. 6. The performance enhancement conferred by the DEP force. (a) Enhancement of the sensitivity with the DEP force for detection of amyloid beta 42 (blue) and PSA protein (green). The improvement of the LOD by the nDEP force in detection of (b) amyloid beta 42 and (c) PSA protein. An inverted triangle indicates the LOD in each condition. (For interpretation of the references to color in this figure legend, the reader is referred to the web version of this article.)

4. Conclusions

In this paper, we have suggested a simple method to improve the performance of a sensor by controlling the nano-molecules with a DEP force, and verified the concept using specific antibody-antigen reactions with two different biomolecules. The DEP force traps or focuses the biomolecules, leading to a change of the binding efficiency between the antibody and target molecules. Consequently, the performance of the sensor is changed. The sensitivity was enhanced by nDEP by about 128% and 258% compared to the reference for amyloid beta 42 and PSA protein detection, respectively. In addition, the LOD was improved by a maximum of 2-orders of magnitude with nDEP. These results confirm the possibility of enhancement of a sensor's performance by achieving control of the biomolecules.

The concept proposed in this paper is clearly a powerful method to improve a sensor's sensitivity and LOD. Moreover, it offers price competitiveness and convenience because this technique can simultaneously induce the DEP signal and measure the change in the reaction signal using a single platform. Although the enhancement of sensitivity is not dramatic since the IME sensor used in this experiment is not suitable for inducing the DEP force, these limitations can be easily overcome by optimizing the structure of the sensor.

Acknowledgements

The authors are grateful for financial support from the KIST institutional Program (2V04870 and 2E26664) and Korea Health Industry Development Institute (KHIDI, HI14C3319).

Appendix A. Supplementary information

Supplementary information associated with this article can be found in the online version at http://dx.doi.org/10.1016/j.bios.2016.06.081.

References

Chen, P., Peng, Y., Hao, Y., Huang, Q., Liu, Y.-N., Deng, C., 2013. Sens. Actuators B: Chem. 183, 589–593.
Dastider, S. G., Barizuddin, S., Yuksek, N., Dweik, M., 2016. In: Proceedings of 2016 IEEE 29th International Conference on Micro Electro Mechanical Systems (MEMS), Shanghai, China.
Derkus, B., 2016. Biosens. Bioelectron. 79, 901–913.
Fang, L., Lib, W., Zhoub, Y., Liua, C.-C., 2009. Sens. Actuators B: Chem. 137, 235–238.
Gerwen, P.V., Laureyn, W., Laureys, W., Huyberechts, G., De Beeck, M.O., Baert, K., Suls, J., Sansen, W., Jacobs, P., Hermans, L., 1998. Sens. Actuators B: Chem. 49, 73–80.
Gong, J.R., 2010. Small 6, 967–973.
Hsueh, H.T., Lin, C.T., 2016. Biosens. Bioelectron. 79, 636–643.
Jin, P.P., Huang, X., Zou, Y.-C., Zhou, L.-J., Wang, X., Zhang, F., Wang, D., Li, G.-D., 2016. Sens. Actuators B: Chem. 224, 381–390.
Jones, T.B., 1995. Electromechanics of Particles. Cambridge University Press,, Cambridge, UK.
Kim, J., Lee, S., Suh, J.-K.F., Park, J.H., Shin, H.-J., 2013. Appl. Phys. Lett. 102, 063105.
Morgan, H., Green, N.G., 2001. Electrokinetic Technologies for Sub-micron Particles. Research Studies Press, Philadelphia, PA.
Ramos, A., Morgan, H., Green, N.G., Castellanos, A., 1998. J. Phys. D: Appl. Phys. 31, 2338–2353.
Song, Y., Luo, N., Zhu, C.Z., Li, H., Du, D., Lin, Y.H., 2016. Biosens. Bioelectron. 76, 195–212.
Zhu, Q., Chai, Y.Q., Zhuo, Y., Yuan, R., 2015. Biosens. Bioelectron. 68, 42–48.